
Bandits with Abstention under Expert Advice

Anonymous Author(s)

Affiliation

Address

email

Abstract

1 We study the classic problem of prediction with expert advice under bandit feedback.
2 Our model assumes that one action, corresponding to the learner’s abstention
3 from play, has no reward or loss on every trial. We propose the *confidence-rated*
4 *bandits with abstentions* (CBA) algorithm, which exploits this assumption to
5 obtain reward bounds that can significantly improve those of the classical EXP4
6 algorithm. Our problem can be construed as the aggregation of confidence-rated
7 predictors, with the learner having the option to abstain from play. We are the
8 first to achieve bounds on the expected cumulative reward for general confidence-
9 rated predictors. In the special case of specialists we achieve a novel reward
10 bound, significantly improving previous bounds of SPECIALISTEXP (treating
11 abstention as another action). We discuss how CBA can be applied to the problem
12 of adversarial contextual bandits with the option of abstaining from selecting any
13 action. We are able to leverage a wide range of inductive biases, outperforming
14 previous approaches both theoretically and in preliminary experimental analysis.
15 Additionally, we achieve a reduction in runtime from quadratic to almost linear in
16 the number of contexts for the specific case of metric space contexts.

17 1 Introduction

18 We study the classic problem of prediction with expert advice under bandit feedback. The problem
19 is structured as a sequence of trials. During each trial, each expert recommends a probability
20 distribution over the set of possible actions. The learner then selects an action, observes, and incurs
21 the (potentially negative) reward associated with that action on that particular trial. In practical
22 applications, errors often lead to severe consequences, and consistently making predictions is neither
23 safe nor economically practical. For this reason, the abstention option has gained a lot of interest
24 in the literature, both in the batch and online setting [Chow, 1957, 1970, Hendrickx et al., 2021,
25 Cortes et al., 2018]. Similarly to previous works, this paper is based on the assumption that one of the
26 actions always has zero reward: such an action is equivalent to an abstention of the learner from play.
27 Besides the rewards being bounded between $[-1, 1]$, we make no additional assumptions regarding
28 how the rewards or expert predictions are generated. In this paper, we present an efficient algorithm
29 CBA (**C**onfidence-rated **B**andits with **A**bstentions) which exploits the abstention action to get reward
30 bounds that can be dramatically higher than those of EXP4 [Auer et al., 2002]. In the worst case, our
31 reward bound essentially matches that of EXP4 so that CBA can be seen as a strict improvement.

32 Our problem can also be seen as that of aggregating *confidence-rated predictors* [Blum and Mansour,
33 2007, Gaillard et al., 2014, Luo and Schapire, 2015] when the learner has the option of abstaining
34 from taking actions. When the problem is phrased in this way, at the start of each trial, each predictor
35 recommends a probability distribution over the actions (which now may not include an action with
36 zero reward) but with a confidence rating. A low confidence rating can mean that either the predictor
37 thinks that all actions are bad (so that the learner should abstain) or simply does not know which

38 action is the best. Previous works on confidence-rated experts measure the performance of their
 39 algorithm in terms of the sum of *scaled* per-trial rewards. In contrast to previous algorithms, our
 40 approach allows for the derivation of bounds on the expected cumulative reward of CBA.

41 This formulation enables us to extend our work to the problem of adversarial contextual bandits with
 42 the abstention option, which has not been studied before. Previous work has considered the abstention
 43 option in the standard (context-free) adversarial bandit setting or in stochastic settings [Cortes et al.,
 44 2018, 2020, Neu and Zivotoskiy, 2020], but not in the contextual and adversarial case. Moreover,
 45 their results and methods cannot be applied to confidence-rated predictors. To get more intuition on
 46 this setup, we can think of any deterministic policy that maps contexts into actions. Any such policy
 47 can be viewed as a classifier, with *foreground* classes associated with each action and a *background*
 48 class associated with abstaining. Our learning bias is represented by a set of information we refer to
 49 as the *basis*, which we formally define later. It encodes contextual structural assumptions that hold
 50 exclusively for the foreground classes and are provided to the algorithm a priori. A particular type
 51 of basis is generated by a set of potential clusters that can overlap. Alternatively, a basis can also
 52 be created using balls generated by any kind of distance function, which groups contexts believed
 53 to be close together. For this latter family of basis, we can also achieve a significant speedup in the
 54 per-trial time complexity of CBA.

55 One specific scenario where prior algorithms can establish cumulative reward bounds is as follows:
 56 on any given trial, the predictors are *specialists* [Freund et al., 1997], having either full confidence
 57 (a.k.a. *awake*) or no confidence (a.k.a. *asleep*). The SPECIALISTEXP algorithm by Herbster et al.
 58 [2021], a bandit version of the standard specialist algorithm, achieves regret bounds with respect
 59 to any subset of specialists where exactly one specialist is awake on each trial. We differ from this
 60 work as abstention is an algorithmic choice. Instead of sleeping in the rounds where the specialist
 61 is not active, the specialist may vote for abstention, which is a proper action of our algorithm. In
 62 Section 5.2, we present an illustrative problem involving learning balls in a space equipped with a
 63 metric. This example demonstrates our capability to significantly improve SPECIALISTEXP, which
 64 treats abstention as just another action when our confidence-rated predictors are indeed specialists.
 65 For this problem, we also present subroutines that significantly speed up CBA.
 66 For a more detailed discussion of related work, refer to Appendix A.

67 2 Problem formulation and notation

68 We consider the classic problem of prediction with expert advice under bandit feedback. In this
 69 problem we have $K + 1$ actions, E experts, and T trials. On each trial t :

- 70 1. Each expert suggests, to the learner, a probability distribution over the $K + 1$ actions.
- 71 2. The learner selects an action a_t .
- 72 3. The reward incurred by action a_t on trial t (which is in $[-1, 1]$ and is selected by Nature
 73 before the trial) is revealed to the learner.

74 The aim of the learner is to maximize the cumulative reward obtained by its selected actions. As
 75 discussed in Section 1, we consider the case in which there is an action (the abstention action) that
 76 incurs zero reward on every trial.

77 We denote our action set by $[K] \cup \{\square\}$ where \square is the abstention action. For each trial $t \in [T]$ we
 78 define the vector $\mathbf{r}_t \in [-1, 1]^K$ such that for all $a \in [K]$, $r_{t,a}$ is the reward obtained by action a on
 79 trial t . Moreover, we define $r_{t,\square} := 0$ which is the reward of the abstention action \square .

80 It will be useful for us to represent probability distributions over the actions by vectors in the set:

$$\mathcal{A} := \{\mathbf{s} \in [0, 1]^K \mid \|\mathbf{s}\|_1 \leq 1\}.$$

81 Any vector $\mathbf{s} \in \mathcal{A}$ represents the probability distribution over actions which assigns, for all $a \in [K]$,
 82 a probability of s_a to action a , and assigns a probability of $1 - \|\mathbf{s}\|_1$ to the abstention action \square , where
 83 $\|\mathbf{s}\|_1$ denotes 1-norm of \mathbf{s} . We write $a \sim \mathbf{s}$ to represent that an action a is drawn from this probability
 84 distribution. We will refer to the elements of the set \mathcal{A} as *stochastic actions*.

85 A *policy* is any element of \mathcal{A}^T (noting that any such policy is a matrix in $[0, 1]^{T \times K}$). Any policy
 86 $\mathbf{e} \in \mathcal{A}^T$ defines a stochastic sequence of actions: on every trial $t \in [T]$ an action $a \in [K] \cup \{\square\}$
 87 being drawn as $a \sim \mathbf{e}_t$. Note that if the learner plays according to a policy $\mathbf{e} \in \mathcal{A}^T$, then on each

88 trial t it obtains an expected reward of $\mathbf{r}_t \cdot \mathbf{e}_t$, where the operator \cdot denotes the dot product. Note that
 89 each expert is equivalent to a policy. Thus, for all $i \in [E]$ we denote the i -th expert by $\mathbf{e}^i \in \mathcal{A}^T$. At
 90 the start of each trial $t \in [T]$, the learner views the sequence $\langle \mathbf{e}_t^i \mid i \in [E] \rangle$.

91 We can also view the experts as *confidence-rated predictors* over the set $[K]$: for each $i \in [E]$ and
 92 $t \in [T]$, the vector \mathbf{e}_t^i can be viewed as suggesting the probability distribution $\mathbf{e}_t^i / \|\mathbf{e}_t^i\|_1$ over $[K]$, but
 93 with confidence $\|\mathbf{e}_t^i\|_1$. We denote this confidence by $c_{t,i} := \|\mathbf{e}_t^i\|_1$ and write $\mathbf{c}_t := (c_{t,1}, \dots, c_{t,E})$.

94 In this work, we will refer to the *unnormalized relative entropy* defined by:

$$\Delta(\mathbf{u}, \mathbf{v}) := \sum_{i \in [E]} u_i \ln \left(\frac{u_i}{v_i} \right) - \|\mathbf{u}\|_1 + \|\mathbf{v}\|_1$$

95 for any $\mathbf{u}, \mathbf{v} \in \mathbb{R}_+^E$. We will also use the Iverson bracket notation $\llbracket \text{PRED} \rrbracket$ as the indicator function,
 96 meaning that it is equal to 1 if PRED is true, and 0 otherwise. All the proofs are in the Appendix.

97 3 Main result

98 Our main result is represented by the bound on the cumulative reward of our algorithm CBA. We
 99 note that any *weight* vector $\mathbf{u} \in \mathbb{R}_+^E$ induces a matrix $\boldsymbol{\pi}(\mathbf{u}) \in \mathbb{R}_+^{T \times K}$ defined by

$$\boldsymbol{\pi}(\mathbf{u}) := \sum_{i \in [E]} u_i \mathbf{e}^i,$$

100 which is the linear combination of the experts with coefficients given by \mathbf{u} . However, only some of
 101 such linear combinations generate valid policies. Thus, we define

$$\mathcal{V} := \{ \mathbf{u} \in \mathbb{R}_+^E \mid \boldsymbol{\pi}(\mathbf{u}) \in \mathcal{A}^T \}$$

102 as the set of all weight vectors that generate valid policies. Particularly, note that $\mathbf{u} \in \mathcal{V}$ if and only
 103 if, on every trial t , the weighted sum of the confidences $\mathbf{u} \cdot \mathbf{c}_t$ is no greater than one. Given some
 104 $\mathbf{u} \in \mathcal{V}$, we define

$$\rho(\mathbf{u}) := \sum_{t \in [T]} \mathbf{r}_t \cdot \boldsymbol{\pi}_t(\mathbf{u}),$$

105 which would be the expected cumulative reward of the learner if it was to follow the policy $\boldsymbol{\pi}(\mathbf{u})$.
 106 We point out that the learner does not know \mathcal{V} or the function $\boldsymbol{\pi}$ a-priori.

107 The following theorem (proved in Appendix B) allows us to bound the regret of CBA with respect to
 108 any valid linear combination \mathbf{u} of experts.

109 **Theorem 3.1.** *CBA takes parameters $\eta \in (0, 1)$ and $\mathbf{w}_1 \in \mathbb{R}_+^E$. For any $\mathbf{u} \in \mathcal{V}$ the expected
 110 cumulative reward of CBA is bounded below by:*

$$\sum_{t \in [T]} \mathbb{E}[r_{t,a_t}] \geq \mathbb{E}[\rho(\mathbf{u})] - \frac{\Delta(\mathbf{u}, \mathbf{w}_1)}{\eta} - \eta(12K + 2)T,$$

111 where the expectations are with respect to the randomization of CBA's strategy. The per-trial time
 112 complexity of CBA is in $\mathcal{O}(KE)$.

113 We now compare our bound to those of previous algorithms. Firstly, EXP4 can only achieve bounds
 114 relative to a $\mathbf{u} \in \mathcal{V}$ with $\|\mathbf{u}\|_1 = 1$, in which case it essentially matches our bound but with $12K + 2$
 115 replaced by $8K + 8$. Hence, for any $\mathbf{u} \in \mathcal{V}$ the EXP4 bound essentially replaces the term $\rho(\mathbf{u})$ in our
 116 bound by $\rho(\mathbf{u}) / \|\mathbf{u}\|_1$. Note that $\|\mathbf{u}\|_1$ could be as high as the number of experts which implies we
 117 can dramatically outperform EXP4¹.

118 When viewing our experts as confidence-rated predictors, we note that previous algorithms for this
 119 setting only give bounds on a weighted sum of the per-trial rewards where the weight on each trial is
 120 $\mathbf{u} \cdot \mathbf{c}_t$ for some $\mathbf{u} \in \mathcal{V}$. This is only a cumulative reward bound when $\mathbf{u} \cdot \mathbf{c}_t = 1$ for all $t \in [T]$, and
 121 finding such a \mathbf{u} is typically impossible. When there does exist \mathbf{u} that satisfies this constraint, the
 122 reward relative to \mathbf{u} is essentially the same as for us [Blum and Mansour, 2007]. However, there will
 123 often be another value of \mathbf{u} that will give us a much better bound, as we show in Section 5.2.

¹Precisely, If for each expert there exists a trial in which the confidence is 1, then we have $0 \leq \|\mathbf{u}\|_1 \leq E$.
 Otherwise can be high as $0 \leq \|\mathbf{u}\|_1 \leq E/c^*$, where $c^* = \max_{t \in [T]} c_t^i$.

Algorithm 1 CBA(w_1, η)

For $t = 1, 2, \dots, T$ **do**:

1. For all $i \in [E]$ receive e_t^i
2. For all $i \in [E]$ set $c_{t,i} \leftarrow \|e_t^i\|_1$
3. **If** $\|c_t\|_1 \leq 1$ **then**:

(a) Set $\tilde{w}_t \leftarrow w_t$

4. **Else**:

(a) By interval bisection find $\lambda > 0$ such that:

$$\sum_{i \in [E]} c_{t,i} w_{t,i} \exp(-\lambda c_{t,i}) = 1$$

(b) For all $i \in [E]$ set $\tilde{w}_{t,i} \leftarrow w_{t,i} \exp(-\lambda c_{t,i})$

5. Set:

$$s_t \leftarrow \sum_{i \in [E]} \tilde{w}_{t,i} e_t^i$$

6. Draw $a_t \sim s_t$

7. Receive r_{t,a_t}

8. For all $a \in [K]$ set:

$$\hat{r}_{t,a} \leftarrow 1 - \mathbb{I}[a = a_t](1 - r_{t,a_t})/s_{t,a_t}$$

9. For all $i \in [E]$ set $w_{(t+1),i} \leftarrow \tilde{w}_{t,i} \exp(\eta e_t^i \cdot \hat{r}_t)$
-

124 4 The CBA algorithm

125 The CBA algorithm is given in Algorithm 1. In this section, we describe its derivation via a
126 modification of the classic *mirror descent* algorithm.

127 Our modification of mirror descent is based on the following mathematical objects. For all $t \in [T]$
128 we first define:

$$\mathcal{V}_t := \{v \in \mathbb{R}_+^E \mid \|\pi_t(v)\|_1 \leq 1\},$$

129 which is the set of all weight vectors that give rise to linear combinations producing valid stochastic
130 actions at trial t . Given some $t \in [T]$, we define our *objective function* $\rho_t : \mathcal{V}_t \rightarrow [-1, 1]$ as

$$\rho_t(v) := r_t \cdot \pi(v) \text{ for all } v \in \mathcal{V}_t.$$

131 Like mirror descent, CBA maintains, on each trial $t \in [T]$, a weight vector $w_t \in \mathbb{R}_+^E$. However,
132 unlike mirror descent on the simplex, we do not keep w_t normalized, but we will instead project it
133 into \mathcal{V}_t at the start of trial t , producing a vector \tilde{w}_t . Also, unlike mirror descent, CBA does not use
134 the actual gradient (which it does not know) of ρ_t at \tilde{w}_t , but (inspired by the EXP3 algorithm) uses
135 an unbiased estimator instead. Specifically, on each trial $t \in [T]$, CBA does the following:

- 136 1. Set $\tilde{w}_t \leftarrow \operatorname{argmin}_{v \in \mathcal{V}_t} \Delta(v, w_t)$.
- 137 2. Randomly construct a vector $g_t \in \mathbb{R}^E$ such that $\mathbb{E}[g_t] = \nabla \rho_t(\tilde{w}_t)$.
- 138 3. Set $w_{t+1} \leftarrow \operatorname{argmin}_{v \in \mathbb{R}_+^E} (\eta g_t \cdot (\tilde{w}_t - v) + \Delta(v, \tilde{w}_t))$.

139 This naturally raises two questions: how is a_t selected and how is g_t constructed? On each trial
140 $t \in [T]$ we define

$$s_t := \sum_{i \in [E]} \tilde{w}_{t,i} e_t^i,$$

141 which is the stochastic action generated by the linear combination \tilde{w}_t , and select $a_t \sim s_t$. Note that:

$$\mathbb{E}[r_{t,a_t}] = \rho_t(\tilde{w}_t), \quad (1)$$

142 which confirms that ρ_t is our objective function at trial t . Once r_{t,a_t} is revealed to us we can proceed
143 to construct the gradient estimator g_t . It is important that we construct this estimator in a specific
144 way. Inspired by EXP4 we first define a reward estimator \hat{r}_t such that for all $a \in [K]$ we have:

$$\hat{r}_{t,a} := 1 - \mathbb{I}[a = a_t](1 - r_{t,a_t})/s_{t,a_t}.$$

145 This reward estimate is unbiased as:

$$\mathbb{E}[\hat{r}_{t,a}] = 1 - \Pr[a = a_t](1 - r_{t,a})/s_{t,a} = r_{t,a}.$$

146 We then define, for all $i \in [E]$, the component:

$$g_{t,i} := \mathbf{e}_t^i \cdot \hat{\mathbf{r}}_t.$$

147 Note that for all $i \in [E]$ we have:

$$\mathbb{E}[g_{t,i}] = \mathbf{e}_t^i \cdot \mathbb{E}[\hat{\mathbf{r}}_t] = \mathbf{e}_t^i \cdot \mathbf{r}_t = \partial_i \rho_t(\tilde{\mathbf{w}}_t)$$

148 so that $\mathbb{E}[\mathbf{g}_t] = \nabla \rho_t(\tilde{\mathbf{w}}_t)$ as required.

149 Now that we defined the process by which CBA operates we must show how to compute $\tilde{\mathbf{w}}_t$ and
 150 \mathbf{w}_{t+1} . First we show how to compute $\tilde{\mathbf{w}}_t$ from \mathbf{w}_t . If $\|\mathbf{c}_t\|_1 \leq 1$ it holds that $\mathbf{w}_t \in \mathcal{V}_t$ so we
 151 immediately have $\tilde{\mathbf{w}}_t = \mathbf{w}_t$. Otherwise we must find $\tilde{\mathbf{w}}_t \in \mathbb{R}_+^E$ that minimizes $\Delta(\tilde{\mathbf{w}}_t, \mathbf{w}_t)$ subject to
 152 the constraint: $\sum_{i \in [E]} \tilde{w}_{t,i} c_{t,i} = 1$, which is equivalent to the constraint that $\|\boldsymbol{\pi}(\tilde{\mathbf{w}}_t)\|_1 = 1$. Hence,
 153 by Lagrange's theorem there exists λ such that:

$$\nabla_{\tilde{\mathbf{w}}_t} \left(\Delta(\tilde{\mathbf{w}}_t, \mathbf{w}_t) + \lambda \sum_{i \in [E]} \tilde{w}_{t,i} c_{t,i} \right) = 0$$

154 which is solved by setting, for all $i \in [E]$:

$$\tilde{w}_{t,i} := w_{t,i} \exp(-\lambda c_{t,i}).$$

155 The constraint is then satisfied if λ is such that:

$$\sum_{i \in [E]} c_{t,i} w_{t,i} \exp(-\lambda c_{t,i}) = 1.$$

156 Since this function is monotonic decreasing, λ can be found by interval bisection.

157 Turning to the computation of \mathbf{w}_{t+1} , since it is unconstrained it is found by the equation:

$$\nabla_{\mathbf{w}_{t+1}} (\mathbf{g}_t \cdot \mathbf{w}_{t+1} + \eta^{-1} \Delta(\mathbf{w}_{t+1}, \tilde{\mathbf{w}}_t)) = 0.$$

158 which is solved by setting, for all $i \in [E]$:

$$w_{(t+1),i} := \tilde{w}_{t,i} \exp(\eta g_{t,i}). \quad (2)$$

159 5 Adversarial contextual bandits with abstention

160 One main application of CBA is in the problem of adversarial contextual bandits with a finite context
 161 set. In this problem, we have a finite set of *contexts* \mathcal{X} . A-priori nature selects a sequence:

$$\langle (x_t, \mathbf{r}_t) \in \mathcal{X} \times [-1, 1]^K \mid t \in [T] \rangle,$$

162 but does not reveal it to the learner. For all $t \in [T]$ we define $r_{t,\square} := 0$. On each trial $t \in [T]$ the
 163 learner observes the context x_t , selects an action $a_t \in [K] \cup \{\square\}$, and sees and incurs the reward
 164 $r_{t,a_t} \in [-1, 1]$.

165 We will assume that we are given, a-priori, a set $\mathcal{B} \subseteq 2^{\mathcal{X}}$ that we call the *basis*. We call each element
 166 of \mathcal{B} a *basis element* (which is a set of contexts). We will later introduce various potential bases,
 167 determined by the nature of the context's structure: points within a metric space, nodes within a
 168 graph, and beyond. Importantly, our method is capable of accommodating any type of basis and, thus,
 169 any potential inductive bias that might be present in the data.

170 Given our basis we run our algorithm CBA with each expert corresponding to a pair $(B, k) \in \mathcal{B} \times [K]$.
 171 The expert corresponding to each pair (B, k) will deterministically choose action k when the current
 172 context x_t is in B , and abstain otherwise. We can therefore state the following theorem (Proved in
 173 Appendix C)

174 **Corollary 5.1.** *Given any basis \mathcal{B} of cardinality N and any $M \in \mathbb{N}$ we can implement CBA*
 175 *such that for any sequence of disjoint basis elements $\langle B_j \mid j \in [M] \rangle$ with corresponding actions*
 176 *$\langle b_j \in [K] \mid j \in [M] \rangle$ we have:*

$$\sum_{t \in [T]} \mathbb{E}[r_{t,a_t}] \geq \sum_{t \in [T]} \sum_{j \in [M]} \mathbb{1}[x_t \in B_j] r_{t,b_j} - \sqrt{2M \ln(N)(6K+1)T}.$$

177 *The per-trial time complexity of this implementation of CBA is in $\mathcal{O}(KN)$.*

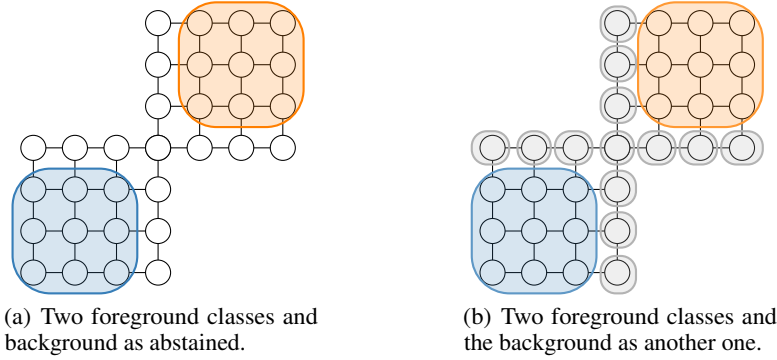


Figure 1: Illustrative example of abstention where we cover the foreground and background classes with metric balls. We consider two clusters (blue and orange) as the foreground and one background class (white), using the shortest path d_∞ metric. Using abstention, we can cover two clusters with one ball for each and abstain the background with no balls required (Fig. 1(a)). In contrast, if we treat the background class as another class, it would require significantly more balls to cover the background class, as seen other 10 gray balls in Fig. 1(b). This increase in the number of balls would lead to a significantly worse bound that involves the number of balls.

178 We briefly comment on the term:

$$\sum_{j \in [M]} \mathbb{1}[x_t \in B_j] r_{t, b_j},$$

179 that appears in the theorem statement. If x_t does not belong to any of the sets in $\langle B_j \mid j \in [M] \rangle$ then
 180 this term is equal to zero (which is the reward of abstaining). Otherwise, since the sets are disjoint,
 181 x_t belongs to exactly one of them and the term is equal to the reward induced by the action that
 182 corresponds to that set. In other words, the total cumulative reward is bounded relative to that of
 183 the policy that abstains whenever x_t is outside the union of the sets and otherwise selects the action
 184 corresponding to the set that x_t lies in.

185 Note the vast improvement of our reward bound over that of SPECIALISTEXP with abstention as one
 186 of the actions. Let's assume our context set is a metric space and our basis is the set of all balls. In
 187 order to get a reward bound for SPECIALISTEXP, the sets in which the specialists are awake must
 188 partition the set \mathcal{X} . This means that we must add to our M balls a disjoint covering (by balls) the
 189 complement of the union of the original M balls. Note that the added balls correspond to the sets
 190 in which the specialists predicting the abstention action are awake. Typically this would require a
 191 huge number of balls so that the total number of specialists is huge (much larger than M); this huge
 192 number of specialists essentially replaces the term M in our reward bound (we illustrate an example
 193 in Figure 1).

194 Furthermore, in Appendix F, we show that the same implementation of CBA is capable of learning a
 195 weighted set of *overlapping* basis elements, as long as the sum of the weights of the basis elements
 196 covering any context is bounded above by one, which SPECIALISTEXP cannot do in general.

197 As we will see below, the practical bases we propose have a moderate size of $|\mathcal{B}| = \mathcal{O}(|\mathcal{X}|^2)$ leading
 198 to a per-step runtime of $\mathcal{O}(K|\mathcal{X}|^2)$ for CBA in this contextual bandit problem. In Section 5.2, we
 199 show how to significantly improve the runtime for a broad family of bases.

200 5.1 A lower bound

201 In this section, we show that CBA is, up to an $\mathcal{O}(\ln(|\mathcal{B}|))$ factor, essentially best possible on this
 202 contextual bandit problem:

203 **Proposition 5.2.** *Take any learning algorithm. Given any basis \mathcal{B} and any $M \in \mathbb{N}$, for any*
 204 *sequence of disjoint basis elements $\langle B_j \mid j \in [M] \rangle$ there exists a sequence of corresponding actions*
 205 *$\langle b_j \in [K] \mid j \in [M] \rangle$ such that an adversary can force:*

$$\sum_{t \in [T]} \sum_{j \in [M]} \mathbb{1}[x_t \in B_j] r_{t, b_j} - \sum_{t \in [T]} \mathbb{E}[r_{t, a_t}] \in \Omega\left(\sqrt{MKKT}\right).$$

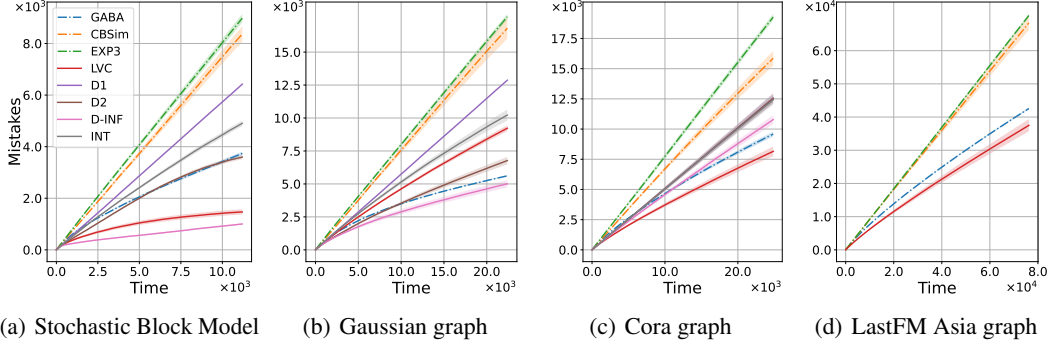


Figure 2: Results regarding the number of mistakes over time. In this context, D1, D2, and D-INF represent the p -norm bases, LVC represents the community detection basis, and INT represents the interval basis. The baselines, EXP3 for each context, Contextual Bandit with similarity, and GABA-II, are denoted as EXP3, CBSim, and GABA, respectively, and are represented with dashed lines.

206 5.2 Efficient learning with balls

207 In practice we can often quantify the similarity between any pair of contexts. That is, the contexts
 208 form a metric space, equipped with a *distance* function $d : \mathcal{X} \times \mathcal{X} \rightarrow \mathbb{R}_+$ known to the learner
 209 a-priori. For example, contexts could have feature vectors in \mathbb{R}^m (and the metric is the standard
 210 Euclidean distance or cosine similarity) or be nodes in a graph with the metric given by the shortest-
 211 path distance. A natural basis for this situation is the set of metric *balls*. Specifically, a ball is any set
 212 $B \subseteq \mathcal{X}$ in which there exists some $x \in \mathcal{X}$ and $\delta \in \mathbb{R}_+$ with:

$$B = \{z \in \mathcal{X} \mid d(x, z) \leq \delta\}.$$

213 For this broad family of bases² we can achieve the following speed-up, relying on a sophisticated
 214 data structure based on binary trees.

215 **Theorem 5.3.** *Let $N := |\mathcal{X}|$. Given any $M \in \mathbb{N}$ we can implement CBA such that for any sequence
 216 of disjoint balls $\langle B_j \mid j \in [M] \rangle$ with corresponding actions $\langle b_j \in [K] \mid j \in [M] \rangle$ we have:*

$$\sum_{t \in [T]} \mathbb{E}[r_{t, a_t}] \geq \sum_{t \in [T]} \sum_{j \in [M]} \mathbb{1}[x_t \in B_j] r_{t, b_j} - \sqrt{4M \ln(N)(6K + 1)T}.$$

217 *The per-trial time complexity of this implementation of CBA is in $\mathcal{O}(KN \ln(N))$.*

218 As there are at most $\mathcal{O}(N^2)$ metric balls, this improves the runtime of the direct CBA implementation
 219 from $\mathcal{O}(KN^2)$ to $\mathcal{O}(KN \ln(N))$, that is almost linear per step. All the details are in Appendix D.

220 6 Preliminary experiments

221 As mentioned above, the bases used in our algorithm can be constructed arbitrarily, allowing to
 222 encompass different inductive biases based on applications. Thus, we consider some representative
 223 bases used on learning tasks on graphs before, each leading to different inductive priors on the
 224 contexts. We provide a short description of the bases here and refer to Appendix G for more details.

Effective p -resistance basis d_p : Balls given by the metric

$$d_p(i, j) := \left(\min_{\substack{\mathbf{u} \in \mathbb{R}^N \\ u_i - u_j = 1}} \sum_{s, t \in V} |u_s - u_t|^p \right)^{-1/p}.$$

225 We use d_1 , d_2 , and d_∞ [Herbster and Lever, 2009].

²Actually, we require a weaker condition. We only use the fact that for each context $z \in \mathcal{X}$ we have a set $\mathcal{B}_z = \{B_1^z, \dots, B_\ell^z\}$ of monotonically increasing basis elements, that is, $B_i^z \subseteq B_j^z$ for $i < j$, and the whole basis is formed by the union of these $\mathcal{B} = \bigcup_{z \in \mathcal{X}} \mathcal{B}_z$.

226 **Louvain method basis (LVC):** Communities returned by the Louvain method [Blondel et al., 2008],
227 processed by the greedy peeling algorithm [Lanciano et al., 2024].

228 **Geodesic intervals basis (INT):** All sets of the form $I(x, y) := \{z \in \mathcal{X} \mid z \text{ is on a shortest } x\text{-}y \text{ path}\}$
229 for all $x, y \in \mathcal{X}$ [Pelayo, 2013, Thiessen and Gärtner, 2021].

230 Let N be the cardinality of $|\mathcal{X}|$. For all three basis types, we immediately get an $\mathcal{O}(KN^2)$ runtime
231 per step of CBA as there are $\mathcal{O}(N^2)$ basis elements. Moreover, for d_p balls and the LVC basis we can
232 use the more efficient $\mathcal{O}(KN \ln N)$ implementation through Theorem 5.3. We empirically evaluate
233 our approach in the context of online multi-class node classification on a given graph with bandit
234 feedback. At each time step, the algorithm is presented with a node chosen uniformly at random and
235 must either predict an action from the set of possible actions $[K]$ or abstain. The node can accept
236 (resulting in a positive reward) or reject (resulting in a negative reward) the suggestion based on its
237 preferred class with a certain probability.

238 We compare our approach CBA using each of these bases on real-world and artificial graphs against
239 the following baselines: an implementation of CONTEXTUALBANDIT from Slivkins [2011], the
240 GABA-II algorithm proposed by Herbster et al. [2021], and an EXP3 instance for each data point.
241 We use the following graphs for evaluation.

242 **Stochastic block model.** This graph, inspired by Holland et al. [1983], is generated by spawning an
243 arbitrary number of disjoint cliques representing the foreground classes. Then an arbitrary number of
244 background points are generated and connected to every possible point with a low probability. In
245 Figure 2(a) are displayed the results for the case of $F = 160$ nodes for each foreground class and
246 $B = 480$ nodes for the background class. Connecting each node of the background class with a
247 probability of $1/\sqrt{FB}$.

248 **Gaussian graph.** The points on this graph are generated in a two-dimensional space using five
249 different Gaussian distributions with zero mean. Four of them are positioned at the corners of the
250 unit square, representing the foreground classes and having a relatively low standard deviation.
251 Meanwhile, the fifth distribution, representing the background class, is centered within the square
252 and is characterized by a larger standard deviation. The points are linked in a k -nearest neighbors
253 graph. In Figure 2(b) are displayed the results for 160 nodes for each foreground class and a standard
254 deviation of 0.2, 480 nodes for the background class with a standard deviation of 1.75, along with a
255 7-nearest neighbors graph.

256 **Real-world dataset.** We tested our approach on the Cora dataset [Sen et al., 2008] and the LastFM
257 Asia dataset [Leskovec and Krevl, 2014]. While both of these graphs contain both features and a
258 graph, we exclusively utilized the largest connected component of each graph, resulting in 2485
259 nodes and 5069 edges for the Cora graph and 7624 nodes and 27806 edges for the LastFM Asia
260 graph. Subsequently, we randomly chose a subset of three out of the original seven and eighteen
261 classes, respectively, to serve as the background class. Additionally, we selected 15% of the nodes
262 from the foreground classes randomly to represent noise points, and we averaged the results over
263 multiple runs, varying the labels chosen for noise. Both in Figures 2(c) and 2(d) we averaged over 5
264 different label sets as noise. For the LastFM Asia graph, we exclusively tested the LVC bases, as it is
265 the most efficient one to compute given the large size of the graph.

266 **Results.** The results from both synthetically generated tests (Figures 2(a) and 2(b)) demonstrate
267 the superiority of our method when compared to the baselines. In particular, d_∞ -balls delivered
268 exceptional results for both graphs, implying that d_∞ -balls effectively cover the foreground classes
269 as expected. For the Cora dataset (Figure 2(c)), we observed that our method outperforms GABA-
270 II only when employing the community detection basis. This similarity in performance is likely
271 attributed to the dataset’s inherent lack of noise. Worth noting that the method we employed to inject
272 noise into the dataset may not have been the optimal choice for this specific context. For the LastFM
273 Asia dataset, our objective was to assess the practical feasibility of the model on a larger graph. We
274 tested the LVC bases as they were the most promising and most efficient to compute. We outperform
275 the baselines in our evaluation as shown in Figure 2(d) and further discussed in Appendix H.

276 In summary, our first results confirm what we expected: our approach excels when we choose basis
277 functions that closely match the context’s structure. However, it also encounters difficulties when the
278 chosen basis functions are not a good fit for the context. In Appendix H, the results for a wide range
279 of different parameters used to generate the previously described graphs are displayed.

280 References

- 281 Morteza Alamgir and Ulrike von Luxburg. Phase transition in the family of p -resistances. In *Proc.*
282 *NIPS*, pages 379–387, 2011.
- 283 Peter Auer and Philip M Long. Structural results about on-line learning models with and without
284 queries. *Mach. Learn.*, 36:147–181, 1999.
- 285 Peter Auer, Nicolò Cesa-Bianchi, Yoav Freund, and Robert E Schapire. The nonstochastic multiarmed
286 bandit problem. *SIAM J. Comput.*, 32(1):48–77, 2002.
- 287 Amir Beck. *First-Order Methods in Optimization*. SIAM, 2017.
- 288 Vincent D Blondel, Jean-Loup Guillaume, Renaud Lambiotte, and Etienne Lefebvre. Fast unfolding
289 of communities in large networks. *J. Stat. Mech. Theory Exp.*, 2008(10):P10008, 2008.
- 290 Avrim Blum and Yishay Mansour. From external to internal regret. *J. Mach. Learn. Res.*, 8(6), 2007.
- 291 Marco Bressan, Nicolò Cesa-Bianchi, Silvio Lattanzi, and Andrea Paudice. Exact recovery of clusters
292 in finite metric spaces using oracle queries. In *Proc. COLT*, 2021.
- 293 C Chow. On optimum recognition error and reject tradeoff. *IEEE Trans. Inf. Theory*, 16(1):41–46,
294 1970.
- 295 Chi-Keung Chow. An optimum character recognition system using decision functions. *IRE Trans.*
296 *Electron. Comput.*, EC-6(4):247–254, 1957.
- 297 Corinna Cortes, Giulia DeSalvo, Claudio Gentile, Mehryar Mohri, and Scott Yang. Online learning
298 with abstention. In *Proc. ICML*, pages 1059–1067, 2018.
- 299 Corinna Cortes, Giulia DeSalvo, Claudio Gentile, Mehryar Mohri, and Ningshan Zhang. Online
300 learning with dependent stochastic feedback graphs. In *Proc. ICML*, pages 2154–2163, 2020.
- 301 Peter G Doyle and J Laurie Snell. *Random Walks and Electric Networks*, volume 22 of *The Carus*
302 *Mathematical Monographs*. American Mathematical Society, 1984.
- 303 Robert W Floyd. Algorithm 97: shortest path. *Commun. ACM*, 5(6):345, 1962.
- 304 Santo Fortunato. Community detection in graphs. *Phys. Rep.*, 486(3):75–174, 2010.
- 305 Yoav Freund, Robert E Schapire, Yoram Singer, and Manfred K Warmuth. Using and combining
306 predictors that specialize. In *Proc. STOC*, pages 334–343, 1997.
- 307 Pierre Gaillard, Gilles Stoltz, and Tim Van Erven. A second-order bound with excess losses. In *Proc.*
308 *COLT*, pages 176–196, 2014.
- 309 Ralph E Gomory and Tien Chung Hu. Multi-terminal network flows. *J. Soc. Ind. Appl. Math.*, 9(4):
310 551–570, 1961.
- 311 Kilian Hendrickx, Lorenzo Perini, Dries Van der Plas, Wannes Meert, and Jesse Davis. Machine
312 learning with a reject option: A survey. *arXiv preprint arXiv:2107.11277*, 2021.
- 313 Mark Herbster and Guy Lever. Predicting the labelling of a graph via minimum p -seminorm
314 interpolation. In *Proc. COLT*, 2009.
- 315 Mark Herbster, Stephen Pasteris, Fabio Vitale, and Massimiliano Pontil. A gang of adversarial
316 bandits. In *Proc. NeurIPS*, pages 2265–2279, 2021.
- 317 Paul W Holland, Kathryn Blackmond Laskey, and Samuel Leinhardt. Stochastic blockmodels: First
318 steps. *Soc. Netw.*, 5(2):109–137, 1983.
- 319 Tommaso Lanciano, Atsushi Miyauchi, Adriano Fazzino, and Francesco Bonchi. A survey on the
320 densest subgraph problem and its variants. *ACM Comput. Surv.*, 56(8):1–40, 2024.
- 321 Tor Lattimore and Csaba Szepesvári. *Bandit Algorithms*. Cambridge University Press, 2020.

- 322 Jure Leskovec and Andrej Krevl. SNAP Datasets: Stanford large network dataset collection. <http://snap.stanford.edu/data>, June 2014.
323
- 324 Haipeng Luo and Robert E Schapire. Achieving all with no parameters: Adanormalhedge. In *Proc.*
325 *COLT*, pages 1286–1304, 2015.
- 326 Gergely Neu and Nikita Zhivotovskiy. Fast rates for online prediction with abstention. In *Proc.*
327 *COLT*, pages 3030–3048, 2020.
- 328 Mark E.J. Newman and Michelle Girvan. Finding and evaluating community structure in networks.
329 *Phys. Rev. E*, 69(2):026113, 2004.
- 330 Ignacio M. Pelayo. *Geodesic Convexity in Graphs*. Springer, 2013.
- 331 Shota Saito and Mark Herbster. Multi-class graph clustering via approximated effective p -resistance.
332 In *Proc. ICML*, pages 29697–29733, 2023.
- 333 Nicolas Schreuder and Evgenii Chzhen. Classification with abstention but without disparities. In
334 *Proc. UAI*, pages 1227–1236, 2021.
- 335 Yevgeny Seldin and Gábor Lugosi. A lower bound for multi-armed bandits with expert advice. In
336 *Proc. EWR*L, volume 2, page 7, 2016.
- 337 Prithviraj Sen, Galileo Namata, Mustafa Bilgic, Lise Getoor, Brian Galligher, and Tina Eliassi-Rad.
338 Collective classification in network data. *AI Mag.*, 29(3):93–93, 2008.
- 339 Aleksandrs Slivkins. Contextual bandits with similarity information. In *Proc. COLT*, pages 679–702,
340 2011.
- 341 Maximilian Thiessen and Thomas Gärtner. Active learning of convex halfspaces on graphs. In *Proc.*
342 *NeurIPS*, 2021.
- 343 Vincent A Traag. Faster unfolding of communities: Speeding up the louvain algorithm. *Phys. Rev. E*,
344 92(3):032801, 2015.
- 345 Marcel LJ van De Vel. *Theory of Convex Structures*. Elsevier, 1993.

346 **A Additional related works**

347 The non-stochastic multi-armed bandit problem, initially introduced by Auer et al. [2002], has been
 348 a subject of significant research interest. Auer et al. [2002] also introduced the multi-armed bandit
 349 problem with expert advice, introducing the EXP4 algorithm. EXP4 evolved the field of multi-armed
 350 bandits to encompass more complex scenarios, particularly the contextual bandit [Lattimore and
 351 Szepesvári, 2020]. Contextual bandits are an extension of the classical multi-armed bandit framework,
 352 where an agent makes a sequence of decisions while taking into account contextual information. We
 353 also mention that our work is also related to the multi-class classification with bandit feedback, called
 354 *weak reinforcement* [Auer and Long, 1999]. An action in our bandit setting corresponds to a class in
 355 the multi-class classification framework.

356 As discussed in the introduction, a key aspect of this work is the option to abstain from making any
 357 decision. In the batch setting [Chow, 1957, 1970], this option is usually referred to as “rejection”.
 358 These works study whether to use or reject a specific model prediction based on specific requests
 359 (see Hendrickx et al. [2021] for a survey). In online learning, “rejection” can be the possibility of
 360 abstention by the learner. These works usually rely on a cost associated with the abstention action.
 361 Neu and Zhivotovskiy [2020] studied the magnitude of the cost associated with abstention in an
 362 expert setting with bounded losses. They state that if the cost is lower than half of the amplitude of
 363 the interval of the loss, it is possible to derive bounds that are independent of the time. In Cortes et al.
 364 [2018], a non-contextual and partial information setting with the option of abstention is studied. The
 365 sequel model [Cortes et al., 2020] regards this model as a special case of their stochastic feedback
 366 graph model. Schreuder and Chzhen [2021] studied the fairness setting when using the option of
 367 abstaining as it may lead to discriminatory predictions.

368 **B CBA analysis**

369 Here we prove Theorem 3.1 from the modification of mirror descent (and the specific construction of
 370 \mathbf{g}_t) given in Section 4. Whenever we take expectations in this analysis they are over the draw of a_t
 371 from \mathbf{s}_t for some $t \in [T]$. As for mirror descent, our analysis hinges on the following classic lemma:

372 **Lemma B.1.** *Given any convex set $\mathcal{C} \subseteq \mathbb{R}_+^E$, any convex function $\xi : \mathbb{R}_+^E \rightarrow \mathbb{R}$, any $\mathbf{q} \in \mathcal{C}$ and any*
 373 *$\mathbf{z} \in \mathbb{R}_+^E$ with:*

$$\mathbf{q} = \operatorname{argmin}_{\mathbf{v} \in \mathcal{C}} (\xi(\mathbf{v}) + \Delta(\mathbf{v}, \mathbf{z})),$$

374 *then for all $\mathbf{u} \in \mathcal{C}$ we have:*

$$\xi(\mathbf{u}) + \Delta(\mathbf{u}, \mathbf{z}) \geq \xi(\mathbf{q}) + \Delta(\mathbf{u}, \mathbf{q}).$$

375 *Proof.* Theorem 9.12 in Beck [2017] shows that the theorem holds if Δ is Bregman divergence. In
 376 our case Δ is indeed a Bregman divergence: that of the convex function $f : \mathbb{R}_+^E \rightarrow \mathbb{R}$ for all $\mathbf{v} \in \mathbb{R}_+^E$
 377 defined by:

$$f(\mathbf{v}) := \sum_{i \in [E]} v_i \ln(v_i),$$

378 which concludes the proof. □

379 Choose any $\mathbf{u} \in \mathcal{V}$ and $t \in [T]$. We immediately have $\mathcal{V} \subseteq \mathcal{V}_t$ by definition, and therefore $\mathbf{u} \in \mathcal{V}_t$.
 380 Hence, by setting ξ such that $\xi(\mathbf{v}) := 0$ for all $\mathbf{v} \in \mathbb{R}_+^E$, setting $\mathcal{C} \in \mathcal{V}_t$ and setting $\mathbf{z} = \mathbf{w}_t$ in Lemma
 381 B.1 we have $\mathbf{q} = \tilde{\mathbf{w}}_t$ so that:

$$\Delta(\mathbf{u}, \mathbf{w}_t) \geq \Delta(\mathbf{u}, \tilde{\mathbf{w}}_t). \tag{3}$$

382 Alternatively, by setting ξ such that $\xi(\mathbf{v}) := \eta \mathbf{g}_t \cdot (\tilde{\mathbf{w}}_t - \mathbf{v})$ for all $\mathbf{v} \in \mathbb{R}_+^E$, setting $\mathcal{C} = \mathbb{R}_+^E$ and
 383 setting $\mathbf{z} = \tilde{\mathbf{w}}_t$ in Lemma B.1 we have $\mathbf{q} = \mathbf{w}_{t+1}$ so that:

$$\eta \mathbf{g}_t \cdot (\tilde{\mathbf{w}}_t - \mathbf{u}) + \Delta(\mathbf{u}, \tilde{\mathbf{w}}_t) \geq \eta \mathbf{g}_t \cdot (\tilde{\mathbf{w}}_t - \mathbf{w}_{t+1}) + \Delta(\mathbf{u}, \mathbf{w}_{t+1}). \tag{4}$$

384 Since $\mathbb{E}[\mathbf{g}_t] = \nabla \rho_t(\tilde{\mathbf{w}}_t)$ and ρ_t is linear we have:

$$\mathbb{E}[\mathbf{g}_t \cdot (\tilde{\mathbf{w}}_t - \mathbf{u})] = \rho_t(\tilde{\mathbf{w}}_t) - \rho_t(\mathbf{u}). \tag{5}$$

385 In what follows we use the fact that for all $x \leq 1$ we have:

$$x(1 - \exp(x)) \geq -2x^2. \tag{6}$$

386 For all $i \in [E]$, we have, by definition, that $g_{t,i} = \mathbf{e}_t^i \cdot \hat{\mathbf{r}}_t$ so by Equation (2) we have:

$$\mathbf{g}_t \cdot (\tilde{\mathbf{w}}_t - \mathbf{w}_{t+1}) = \sum_{i \in [E]} \tilde{w}_{t,i} \mathbf{e}_t^i \cdot \hat{\mathbf{r}}_t (1 - \exp(\eta \mathbf{e}_t^i \cdot \hat{\mathbf{r}}_t)).$$

387 Since, for all $a \in [K]$, we have $\hat{r}_{t,a} \leq 1$ and hence, as $\eta < 1$ and, for all $i \in [E]$ we have $\|\mathbf{e}_t^i\|_1 \leq 1$,
388 we can invoke Equation (6), which gives us:

$$\eta \mathbf{g}_t \cdot (\tilde{\mathbf{w}}_t - \mathbf{w}_{t+1}) \geq -2 \sum_{i \in [E]} \tilde{w}_{t,i} (\eta \mathbf{e}_t^i \cdot \hat{\mathbf{r}}_t)^2. \quad (7)$$

389 By definition of $\hat{\mathbf{r}}_t$ we have, for all $i \in [E]$, that:

$$\mathbf{e}_t^i \cdot \hat{\mathbf{r}}_t = \|\mathbf{e}_t^i\|_1 + e_{t,a_t}^i (1 - r_{t,a_t}) / s_{t,a_t} \leq c_{t,i} + 2e_{t,a_t}^i / s_{t,a_t}$$

390 so that since, for all $a \in [K]$, we have $\Pr[a_t = a] = s_{t,a}$ we also have:

$$\mathbb{E}[(\mathbf{e}_t^i \cdot \hat{\mathbf{r}}_t)^2] \leq c_{t,i}^2 + \sum_{a \in [K]} (2e_{t,a}^i c_{t,i} + 4(e_{t,a}^i)^2 / s_{t,a}). \quad (8)$$

391 Since, for all $i \in [E]$ and $a \in [K]$, we have $e_{t,a}^i \leq 1$ and $c_{t,i} \leq 1$ and hence also $c_{t,i}^2 \leq c_{t,i}$ we then
392 have:

$$\mathbb{E}[(\mathbf{e}_t^i \cdot \hat{\mathbf{r}}_t)^2] \leq (2K + 1)c_{t,i} + 4 \sum_{a \in [K]} e_{t,a}^i / s_{t,a}. \quad (9)$$

393 Note that since $\tilde{\mathbf{w}}_t \in \mathcal{V}_t$ we have:

$$\sum_{i \in [E]} \tilde{w}_{t,i} c_{t,i} \leq 1. \quad (10)$$

394 Also, by definition of \mathbf{s}_t we have:

$$\sum_{i \in [E]} \tilde{w}_{t,i} \sum_{a \in [K]} e_{t,a}^i / s_{t,a} = \sum_{a \in [K]} \frac{1}{s_{t,a}} \sum_{i \in [E]} \tilde{w}_{t,i} e_{t,a}^i = \sum_{a \in [K]} \frac{1}{s_{t,a}} s_{t,a} = K. \quad (11)$$

395 Multiplying Inequality (9) by $\tilde{w}_{t,i}$, summing over all $i \in [E]$, and then substituting in Inequality
396 (10) and Equation (11) gives us:

$$\sum_{i \in [E]} \tilde{w}_{t,i} \mathbb{E}[(\mathbf{e}_t^i \cdot \hat{\mathbf{r}}_t)^2] \leq (2K + 1) + 4K = 6K + 1. \quad (12)$$

397 Taking expectations on Inequality (7) and substituting in Inequality (12) (after taking expectations)
398 gives us:

$$\mathbb{E}[\eta \mathbf{g}_t \cdot (\tilde{\mathbf{w}}_t - \mathbf{w}_{t+1})] \geq -\eta^2 (12K + 2). \quad (13)$$

399 Taking expectations (over the draw $a_t \sim \mathbf{s}_t$) on Inequality (4), substituting in Inequalities (3), (5)
400 and (13), and then rearranging gives us:

$$\Delta(\mathbf{u}, \mathbf{w}_t) - \mathbb{E}[\Delta(\mathbf{u}, \mathbf{w}_{t+1})] \geq \eta(\rho_t(\mathbf{u}) - \rho_t(\tilde{\mathbf{w}}_t)) - \eta^2(12K + 2).$$

401 Summing this inequality over all $t \in [T]$, taking expectations (over the entire sequence of action
402 draws) and noting that $\Delta(\mathbf{u}, \mathbf{w}_{T+1}) > 0$ gives us:

$$\Delta(\mathbf{u}, \mathbf{w}_1) \geq \eta \sum_{t \in [T]} \mathbb{E}[\rho_t(\mathbf{u}) - \rho_t(\tilde{\mathbf{w}}_t)] - \eta^2(12K + 2)T.$$

403 Substituting in Equation (1) and rearranging then gives us, by definition of ρ and ρ_t , the required
404 goal:

$$\sum_{t \in [T]} \mathbb{E}[r_{t,a_t}] \geq \mathbb{E}[\rho(\mathbf{u})] - \Delta(\mathbf{u}, \mathbf{w}_1) / \eta - \eta(12K + 2)T.$$

405 ■

406 **C Corollary proof**

407 **Corollary C.1.** *Given any basis \mathcal{B} of cardinality N and any $M \in \mathbb{N}$ we can implement CBA*
 408 *such that for any sequence of disjoint basis elements $\langle B_j \mid j \in [M] \rangle$ with corresponding actions*
 409 *$\langle b_j \in [K] \mid j \in [M] \rangle$ we have:*

$$\sum_{t \in [T]} \mathbb{E}[r_{t,a_t}] \geq \sum_{t \in [T]} \sum_{j \in [M]} \mathbb{1}[x_t \in B_j] r_{t,b_j} - \sqrt{2M \ln(N)(6K+1)T}.$$

410 *The per-trial time complexity of this implementation of CBA is in $\mathcal{O}(KN)$.*

411 *Proof.* The choice of experts for CBA that leads to Theorem 5.1 is defined by the set of pairs so that
 412 $E = N^2K$ and for each $B \in \mathcal{B}$ and action $a \in [K]$ there exists a unique $i \in [E]$ such that for all
 413 $t \in [T]$ and $b \in [K]$ we have:

$$e_{t,b}^i := \mathbb{1}[x_t \in B] \mathbb{1}[b = a].$$

414 By choosing $w_{1,i} = M/N^2$ for all $i \in [E]$, and choosing

$$\eta := (M \ln(N)/(6K+1)T)^{-1/2},$$

415 Theorem 3.1 implies the reward bound in Corollary 5.1. The per-trial time complexity of a direct
 416 implementation of CBA for this set of experts would be $\mathcal{O}(KN)$. \square

417 **D Efficient implementation proof**

418 We here prove the time complexity of Theorem 5.3. The per-trial time complexity of a direct
 419 implementation of CBA for this set of experts would be $\mathcal{O}(KN^2)$. We now show how to implement
 420 CBA in a per-trial time of only $\mathcal{O}(KN \ln(N))$. To do this first note that we can assume, without loss
 421 of generality, that for all $q, x, z \in \mathcal{X}$ with $x \neq z$ we have $d(q, x) \neq d(q, z)$ since ties can be broken
 422 arbitrarily and balls can be duplicated.

423 Given $x, z \in \mathcal{X}$, $a \in [K]$ and $t \in [T]$ we let $y_{t,a}(x, z) := w_{t,i}$ and $\tilde{y}_{t,a}(x, z) := \tilde{w}_{t,i}$ where i is the
 424 index of the expert corresponding to the ball-action pair with ball: $\{q \in \mathcal{X} \mid d(x, q) \leq d(x, z)\}$, and
 425 action a . Given $x, z \in \mathcal{X}$ let $\mathcal{E}(x, z) := \{q \in \mathcal{X} \mid d(x, q) \geq d(x, z)\}$. It is straightforward to derive
 426 the following equations for the quantities in CBA at trial $t \in [T]$. First we have:

$$\|\mathbf{c}_t\|_1 = \sum_{a \in [K]} \sum_{x \in \mathcal{X}} \sum_{z \in \mathcal{E}(x, x_t)} y_{t,a}(x, z).$$

427 For all $x, z \in \mathcal{X}$ and $a \in [K]$ we have the following:

- 428 • If $\|\mathbf{c}_t\|_1 \leq 1$ or $z \notin \mathcal{E}(x, x_t)$ then $\tilde{y}_{t,a}(x, z) = y_{t,a}(x, z)$.
- 429 • If $\|\mathbf{c}_t\|_1 > 1$ and $z \in \mathcal{E}(x, x_t)$ then $\tilde{y}_{t,a}(x, z) = y_{t,a}(x, z) / \|\mathbf{c}_t\|_1$.

430 For all $a \in [K]$ we have:

$$s_{t,a} = \sum_{x \in \mathcal{X}} \sum_{z \in \mathcal{E}(x, x_t)} \tilde{y}_{t,a}(x, z).$$

431 Finally, for all $x, z \in \mathcal{X}$ and $a \in [K]$ we have the following:

$$y_{(t+1),a}(x, z) = \begin{cases} \tilde{y}_{t,a}(x, z) & \text{if } z \notin \mathcal{E}(x, x_t), \\ \tilde{y}_{t,a}(x, z) \exp(\eta e_t^i \cdot \hat{\mathbf{r}}_t) & \text{if } z \in \mathcal{E}(x, x_t). \end{cases}$$

432 Hence, to implement CBA we need, for each $x \in \mathcal{X}$ and $a \in [K]$, a data structure that implicitly
 433 maintains a function $h : \mathcal{X} \rightarrow \mathbb{R}^+$ and has the following two subroutines, that take parameters $q \in \mathcal{X}$
 434 and $p \in \mathbb{R}_+$.

- 435 1. QUERY(q): Compute $\sum_{z \in \mathcal{E}(x, q)} h(z)$.
- 436 2. UPDATE(q, p): Set $h(z) \leftarrow ph(z)$ for all $z \in \mathcal{E}(x, q)$.

Algorithm 2 QUERY(q)

1. For all $i \in [n] \cup \{0\}$ let γ_i be the ancestor of q at depth i in \mathcal{D}
 2. Set $\sigma_n \leftarrow \psi(\gamma_n)\phi(\gamma_n)$
 3. Climb \mathcal{D} from γ_{n-1} to γ_0 . When at γ_i do as follows:
 - (a) If $\gamma_{i+1} = \triangleleft(\gamma_i)$ then set $\sigma_i \leftarrow \phi(\gamma_i)(\sigma_{i+1} + \psi(\triangleright(\gamma_i))\phi(\triangleright(\gamma_i)))$
 - (b) If $\gamma_{i+1} = \triangleright(\gamma_i)$ then set $\sigma_i \leftarrow \phi(\gamma_i)\sigma_{i+1}$
 4. Return σ_0
-

Algorithm 3 UPDATE(q, p)

1. For all $i \in [n] \cup \{0\}$ let γ_i be the ancestor of q at depth i in \mathcal{D}
 2. Descend \mathcal{D} from γ_0 to γ_{n-1} . When at γ_i set:
 - (a) $\phi(\triangleleft(\gamma_i)) \leftarrow \phi(\gamma_i)\phi(\triangleleft(\gamma_i))$
 - (b) $\phi(\triangleright(\gamma_i)) \leftarrow \phi(\gamma_i)\phi(\triangleright(\gamma_i))$
 - (c) $\phi(\gamma_i) \leftarrow 1$
 3. For all $i \in [n-1] \cup \{0\}$, if $\gamma_{i+1} = \triangleleft(\gamma_i)$ then set $\phi(\triangleright(\gamma_i)) \leftarrow p\phi(\triangleright(\gamma_i))$
 4. Set $\phi(\gamma_n) \leftarrow p\phi(\gamma_n)$
 5. Climb \mathcal{D} from γ_{n-1} to γ_0 . When at γ_i set:
 $\psi(\gamma_i) \leftarrow \psi(\triangleleft(\gamma_i))\phi(\triangleleft(\gamma_i)) + \psi(\triangleright(\gamma_i))\phi(\triangleright(\gamma_i))$
-

437 Now fix $x \in \mathcal{X}$ and $a \in [K]$. Let h be as above. On each trial $t \in [T]$ and for all $z \in \mathcal{X}$, $h(z)$ will
438 start equal to $y_{t,a}(x, z)$ and change to $\tilde{y}_{t,a}(x, z)$ and then $y_{(t+1),a}(x, z)$ by applying the UPDATE
439 subroutine.

440 We now show how to implement these subroutines implicitly in a time of $\mathcal{O}(\ln(N))$ as required.
441 Without loss of generality, assume that $N = 2^n$ for some $n \in \mathbb{N}$. Our data structure is based on a
442 balanced binary tree \mathcal{D} whose leaves are the elements of \mathcal{X} in order of increasing distance from x .
443 This implies that for any $z \in \mathcal{X}$ we have that $\mathcal{E}(x, z)$ is the set of leaves that do not lie on the left of
444 z . Given a node $v \in \mathcal{D}$ we let $\uparrow(v)$ be the set of ancestors of v and let $\downarrow(v)$ be the set of all $z \in \mathcal{X}$
445 which are descendants of v . For any internal node v let $\triangleleft(v)$ and $\triangleright(v)$ be the left and right children of
446 v respectively.

447 We maintain functions $\phi, \psi : \mathcal{D} \rightarrow \mathbb{R}_+$ such that for all $v \in \mathcal{D}$ we have:

$$\psi(v) \prod_{v' \in \uparrow(v)} \phi(v') = \sum_{z \in \downarrow(v)} h(z). \quad (14)$$

448 The pseudo-code for the subroutines QUERY and UPDATE are given in Algorithms 2 and 3 respectively.
449 We now prove their correctness. We first consider the QUERY subroutine with parameter $q \in \mathcal{X}$.
450 From Equation (14) we see that, by (reverse) induction on $i \in [n] \cup \{0\}$, we have:

$$\sigma_i \prod_{v' \in \uparrow(\gamma_i) \setminus \{\gamma_i\}} \phi(v') = \sum_{z \in \downarrow(\gamma_i) \cap \mathcal{E}(x, q)} h(z).$$

451 Since γ_0 is the root of \mathcal{D} , we have $\sigma_0 = \sum_{z \in \mathcal{E}(x, q)} h(z)$ as required. Now consider the UPDATE
452 subroutine with parameters $q \in \mathcal{X}$ and $p \in \mathbb{R}_+$. Let h be the implicitly maintained function before
453 the subroutine is called. For Equation (14) to hold after the subroutine is called we need:

$$\psi(v) \prod_{v' \in \uparrow(v)} \phi(v') = \sum_{z \in \downarrow(v)} h'(z). \quad (15)$$

454 where for all $z \in \mathcal{X}$ we have:

$$h'(z) := \llbracket z \notin \mathcal{E}(x, q) \rrbracket h(z) + \llbracket z \in \mathcal{E}(x, q) \rrbracket ph(z).$$

455 We shall now show that Equation (15) does indeed hold after the subroutine is called, which will
456 complete the proof. To show this we consider each step of the subroutine in turn. After Step 2 we
457 have (via induction) that:

- 458 • For all $v \in \uparrow(q)$ we have $\phi(v) = 1$.

459 • For all $v \in \mathcal{D} \setminus \uparrow(q)$ we have:

$$\psi(v) \prod_{v' \in \uparrow(v)} \phi(v') = \sum_{z \in \Downarrow(v)} h(z).$$

460 So, since $\mathcal{E}(x, q)$ is the set of all $z \in \mathcal{X}$ that do not lie to the left of q in \mathcal{D} we have that, after Step 4
461 of the algorithm, the following holds:

- 462 • For all $v \in \uparrow(q)$ we have $\phi(v) = 1$,
463 • For all $v \in \mathcal{D} \setminus \uparrow(q)$ we have:

$$\psi(v) \prod_{v' \in \uparrow(v)} \phi(v') = \sum_{z \in \Downarrow(v)} h'(z).$$

464 Hence, by induction, we have that, after Step 5 of the algorithm, it is the case that for all $v \in \uparrow(q)$ we
465 have: $\psi(v) = \sum_{z \in \Downarrow(v)} h'(z)$. So since $\phi(v) = 1$ for all $v \in \uparrow(q)$ and Step 5 does not alter $\phi(v)$ or
466 $\psi(v)$ for any $v \in \mathcal{D} \setminus \uparrow(q)$ we have Equation (15). ■

467 E Lower bound proof

468 **Proposition E.1.** *Take any learning algorithm. Given any basis \mathcal{B} and any $M \in \mathbb{N}$ then for any*
469 *sequence of disjoint basis elements $\langle \mathcal{B}_j \mid j \in [M] \rangle$ there exists a sequence of corresponding actions*
470 *$\langle b_j \in [K] \mid j \in [M] \rangle$ such that an adversary can force:*

$$\sum_{t \in [T]} \sum_{j \in [M]} \mathbb{1}[x_t \in \mathcal{B}_j] r_{t, b_j} - \sum_{t \in [T]} \mathbb{E}[r_{t, a_t}] \in \Omega(\sqrt{MK T})$$

471 *Proof.* In this scenario, at each time step, either a single expert (i.e., the basis element containing the
472 current context x_t) is active, making predictions based on its label, or no expert is active, prompting
473 the learner to abstain and thus incur zero reward or cost.

474 Therefore we define $T' = \{t \in [T] \mid \sum_{j \in [M]} \mathbb{1}[x_t \in \mathcal{B}_j] = 1\}$ as the set of timesteps in which the
475 learner is going to play. Since the concept of abstention is that our algorithm is not going to pay
476 anything for the timesteps in which we abstain, we can see that:

$$\sum_{t \in [T]} \sum_{j \in [M]} \mathbb{1}[x_t \in \mathcal{B}_j] r_{t, b_j} - \sum_{t \in [T]} \mathbb{E}[r_{t, a_t}] = \sum_{t \in T'} r_{t, b_j} - \sum_{t \in T'} \mathbb{E}[r_{t, a_t}],$$

477 For any ball $j \in [M]$, we define $T_j = \{t \in [T'] \mid \mathbb{1}[x_t \in \mathcal{B}_j]\}$. Following the ideas of Seldin
478 and Lugosi [2016], for any of the sets T_j we can create a multi-armed bandit instance as the one
479 described in the lower bound by Auer et al. [2002]. Note that in the lower bound construction, the
480 abstention arm would be a forehand known suboptimal arm, which results in a lower bound of the
481 order $c\sqrt{(K-1)T}$, for the constant $c = \frac{\sqrt{2}-1}{\sqrt{32 \ln(4/3)}} > 0$. Since the presented context x_t is chosen
482 adversarially at each time step, we can ensure that each basis element is activated for $|T'|/M$ time
483 steps, obtaining:

$$\begin{aligned} \sum_{j \in [M]} \left(\sum_{s \in T'_j} r_{s, b_j} - \sum_{s \in T'_j} \mathbb{E}[r_{s, a_s}] \right) &\geq \sum_{j \in [M]} c\sqrt{(K-1)|T'_j|} \\ &= \sum_{j \in [M]} c\sqrt{(K-1)|T'|/M} \\ &= c\sqrt{M(K-1)|T'|} \end{aligned}$$

484 As we can choose $|T'|$ to be any fraction of T , we end up with the desired lower bound of the order
485 $\Omega(\sqrt{MK T})$, which matches, up to logarithmic factors, the cumulative reward bound presented in
486 Theorem 5.3. □

487 F Overlapping balls extension

488 In this section, we present the theorem that allows us to present the results of overlapping balls as
 489 expressed in Section 5.2. Note that Theorem 5.3 is the special case of Theorem F.1 when the balls are
 490 disjoint and $u_j = 1$ for all $j \in [M]$.

491 **Theorem F.1.** *Let $M \in \mathbb{N}$ and $\{(B_j, b_j, u_j) \mid j \in [M]\}$ be any sequence such that B_j is a ball,
 492 $b_j \in [K]$ is an action, and $u_j \in [0, 1]$ is such that for all $x \in \mathcal{X}$ we have:*

$$\sum_{j \in [M]} \mathbb{1}[x \in B_j] u_j \leq 1.$$

493 For all $t \in [T]$ define:

$$r_t^* := \sum_{j \in [M]} \mathbb{1}[x_t \in B_j] u_j r_{t, b_j},$$

494 which represents the reward of the policy induced by $\{(B_j, b_j, u_j) \mid j \in [M]\}$ on trial t . The regret
 495 of CBA, with the set of experts given in Section 5.2 and with correctly tuned parameters, is then
 496 bounded by:

$$\sum_{t \in [T]} r_t^* - \sum_{t \in [T]} \mathbb{E}[r_{t, a_t}] \in \mathcal{O} \left(\sqrt{\ln(KN)KT \sum_{j \in [M]} u_j} \right).$$

497 Its per-trial time complexity is:

$$\mathcal{O}(KN \ln(N)).$$

498 *Proof.* Direct from Theorem 3.1 using the experts (with efficient implementation) given in Section
 499 5.2 □

500 G The details of the graph bases

501 This section expands the definition and explanations for the bases we used in the Experiment.
 502 Remember that we refer to any set of experts that correspond to set-action pairs of the form $(B, k) \in$
 503 $2^{\mathcal{X}} \times [K]$ as a *basis elements*, and a set of basis elements as *basis*.

504 G.1 p -seminorm balls on graphs

505 As we see in Sec. 5.2, the CBA seems to work only for vector data. However, in the following
 506 sections, we explore how our CBA algorithm can be applied to graph data by creating a ball structure
 507 over the graph.

508 We first introduce the notations of a graph. A graph is a pair of *nodes* $V := [N]$ and *edges* E . An
 509 edge connects two nodes, and we assume that our graph is *undirected* and *weighted*. For each edge
 510 $\{i, j\} \in E$, we denote its weight by c_{ij} . For convenience, for each pair of nodes i, j with $\{i, j\} \notin E$,
 511 we define $c_{ij} = 0$.

512 To form a ball over a graph, a family of metrics we are particularly interested in is given by p -norms
 513 on a given graph G . Let

$$d_p(i, j) := \left(\min_{\substack{\mathbf{u} \in \mathbb{R}^N \\ u_i - u_j = 1}} \sum_{s, t \in V} c_{st} |u_s - u_t|^p \right)^{-1/p}. \quad (16)$$

514 which is a well-defined metric for $p \in [1, \infty)$ if the graph is connected and may be defined for $p = \infty$
 515 by taking the appropriate limits. When $p = 2$ this is the square root of the *effective resistance* circuit
 516 between nodes i and j which comes from interpreting the graph as an electric circuit where the
 517 edges are unit resistors and the denominator of Equation (16) is the power required to maintain a
 518 unit voltage difference between u and v [Doyle and Snell, 1984]. More generally, $d_p(i, j)^p$ is known
 519 as p -(effective) resistance [Herbster and Lever, 2009, Alamgir and von Luxburg, 2011, Saito and
 520 Herbster, 2023]. When $p \in \{1, 2, \infty\}$ there are natural interpretation of the p -resistance. In the case
 521 of $p = 1$, we have that the effective is equal to one over the number of edge-disjoint paths between i

522 and j which is equivalently one over the minimal cut that separates i from j . When $p = 2$ it is the
523 effective resistance as discussed above. And finally when $p = \infty$ we have that d_∞ is the geodesic
524 distance (shortest path) between i and j . Note that, interestingly, there are at most $2N$ distinct balls
525 for d_1 ; as opposed to the general bound $O(N^2)$ on the number of metric balls. This follows since
526 d_1 is an *ultrametric*. A nice feature of metric balls is that they are ordinal, i.e., we can take an
527 increasing function of the distance and the distinct are unchanged. The time complexity for each
528 ball is as follows. For d_1 ball, we compute every pair of distance in $O(N^3)$ using the Gomory-Hu
529 tree [Gomory and Hu, 1961]. For d_2 ball, it is actually enough to compute the pseudoinverse of graph
530 Laplacian once, which costs $O(N^3)$ [Doyle and Snell, 1984]. For d_∞ ball, we can compute every
531 pair of distance in $O(N^3)$ by Floyd–Warshall algorithm [Floyd, 1962].

532 G.2 Community detection bases

533 In this section, we consider only bases formed via a set of subsets (a.k.a clusters) $C \subseteq 2^{[N]}$. Each of
534 these subsets induces K basis elements: one for each action $a \in [K]$. Specifically, the basis element
535 $\beta : [N] \rightarrow [K_\square]$ corresponding to the pair (C, a) is such that $\beta(x)$ is equal to a whenever $x \in C$ and
536 equal to \square otherwise. Hence, in this section, we equate a basis with a set of subsets of $[N]$.

537 We can compute a basis for a given graph $G = (V, E)$ using community detection algorithms.
538 Community detection is one of the most well-studied operations for graphs, where the goal is to
539 find a partition $\{C_1, \dots, C_q\}$ of V (i.e., $\bigcup_{i=1}^q C_i = V$ and $C_i \cap C_j = \emptyset$ for $i \neq j$) so that each C_i
540 is densely connected internally but sparsely connected to the rest of the graph [Fortunato, 2010].
541 There are many community detection algorithms, all of which can be used here, but the most popular
542 algorithm is the Louvain method [Blondel et al., 2008]. We briefly describe how this algorithm works.
543 The algorithm starts with an initial partition $\{\{v\} \mid v \in V\}$ and aggregates the clusters iteratively:
544 For each $v \in V$, compute the gain when moving v from its current cluster to its neighbors’ clusters
545 and indeed move it to a cluster with the maximum gain (if the gain is positive). Note that the gain is
546 evaluated using *modularity*, i.e., the most popular quality function for community detection [Newman
547 and Girvan, 2004]. The algorithm repeats this process until no movement is possible. Then the
548 algorithm aggregates each cluster to a single super node (with appropriate addition of self-loops and
549 change of edge weights) and repeats the above process on the coarse graph as long as the coarse
550 graph is updated. Finally, the algorithm outputs the partition of V in which each cluster corresponds
551 to each super node in the latest coarse graph. Note that it is widely recognized that the Louvain
552 method works in $O(N \log N)$ in practice [Traag, 2015].

553 To obtain a finer-grained basis, we apply the so-called greedy peeling algorithm for each C_i in the
554 output of the Louvain method. For $C_i \subseteq V$ and $v \in C_i$, we denote by $d_{C_i}(v)$ the degree of v in
555 the induced subgraph $G[C_i]$. For $G[C_i]$, the greedy peeling iteratively removes a node with the
556 smallest degree in the currently remaining graph and obtains a sequence of node subsets from C_i to a
557 singleton. Specifically, it works as follows: Set $j \leftarrow |C_i|$ and $C_i^{(j)} \leftarrow C_i$. For each $j = |C_i|, \dots, 2$,
558 compute $v_{\min} \in \arg \min \{d_{C_i^{(j)}}(v) \mid v \in C_i^{(j)}\}$ and $C_i^{(j-1)} \leftarrow C_i^{(j)} \setminus \{v_{\min}\}$. Using a sophisticated
559 data structure, this algorithm runs in linear time [Lanciano et al., 2024].

560 In summary, our community detection basis is the collection of node subsets $\{C_i^{(j)} \mid i = 1, \dots, q, j =$
561 $1, \dots, |C_i|\}$ together with $\{\{v\} \mid v \in V\}$ for completeness.

562 G.3 Graph convexity bases

563 An alternative to metric balls and communities are, for example, (geodesically) convex sets in a
564 graph. They correspond to the inductive bias that if two nodes prefer the same action, then also the
565 nodes on a shortest path between the two tend to prefer the same action. Geodesically convex sets are
566 well-studied [van De Vel, 1993, Pelayo, 2013] and have been recently used in various learning settings
567 on graphs [Bressan et al., 2021, Thiessen and Gärtner, 2021]. Similarly to convex sets in the Euclidean
568 space, a set C of nodes is *convex* if the nodes of any shortest path with endpoints in C are in C , as well.
569 More formally, the (geodesic) *interval* $I(u, v) = \{x \in V : x \text{ is on a shortest path between } u \text{ and } v\}$
570 of two nodes u and v contains all the nodes on a shortest path between them. For a set of node A we
571 define $I(A) = \bigcup_{a, b \in A} I(a, b)$ as a shorthand notation for the union of all pairwise intervals in A . A
572 set A is (geodesically) convex iff $I(A) = A$ and the *convex hull* $\text{conv}(A)$ of a set A is the (unique)
573 smallest convex set containing A . Note that for $u, v \in V$, $I(u, v)$ and $\text{conv}(\{u, v\})$ are typically

574 different sets. Indeed, $I(u, v)$ is in general non-convex, as nodes on a shortest path between two
575 nodes in $I(u, v)$ (except for u, v) are not necessarily contained in $I(u, v)$. As the total number of
576 convex sets can be exponential in N , e.g., all subsets of a complete subgraph are convex, we consider
577 the basis consisting of all intervals: $I(u, v)$ for $u, v \in [N]$. This involves $\mathcal{O}(N^2)$ basis elements, each
578 of size $\mathcal{O}(N)$. With a simple modification of the Floyd Warshall [Floyd, 1962] algorithm, computing
579 the interval basis takes $\mathcal{O}(N^3)$ time complexity.

580 H Additional experimental results

581 We thoroughly explored various configurations for the three graphs described in our experimental
582 setup in Section 6. We run our experiments with an Intel Xeon Gold 6312U processor and 256 GB of
583 RAM ECC 3200 MHz. Figure 3 displays different settings for the number of nodes in each clique
584 and noise levels.

585 As we compare the computational complexity of each basis in Section G and the main results, the
586 most intense computational load in the experiments will arise from the calculation of the basis,
587 which can be seen as an initialization step in our algorithm. The proposed methods have varying
588 computational complexities, and an arbitrarily complex function can be employed to compute the
589 basis. Remark that, in the usual complexity comparison among online learning algorithms using
590 experts, we compare the complexity *given* the experts. Practically, we use pre-computed bases or
591 even human experts. Also note that due to the expensive complexity of the p -balls and the convex
592 sets seen in Section G, we only conduct the LVC for LastFM Asia.

593 In Figure 4, we present multiple settings for generating the Gaussian graph. Here the title of each
594 plot is “Foreground x, y ; Background x', y' ; k -NN,” which is explained as follows: x represents the
595 number of nodes in each foreground class, x' represents the number of nodes in the background class,
596 y represents the standard deviation of the Gaussians generating the foreground class, y' represents
597 the standard deviation of the Gaussian generating the background class, and k represents the number
598 of nearest neighbors used to generate the graph.

599 In Figure 5, we present the various labels chosen as noise for the Cora graph. In Figure 2(c), we
600 presented the averages of all these different configurations. Here, we can see that the main behavior
601 of the various bases is roughly maintained independently of the different labels chosen to be masked
602 as background class.

603 In Figure 6, we present the various labels chosen as noise for the LastFM Asia graph. This graph
604 comprises nodes representing LastFM users in Asian countries and edges representing mutual follower
605 connections. Vertex features are extracted based on the artists liked by the users. During this initial
606 analysis, we arbitrarily chose three out of eighteen possible labels to serve as the background class.
607 In Figure 2(d), we presented the averages of all these different configurations. Varying the chosen
608 background classes also produces different results, this is indeed due to the inherent lack of noise in
609 the dataset. It is nice to see that regardless of the noise labels chosen, the behavior of our algorithm is
610 always good, showing, as expected, that based on the amount of noise, we can just improve.

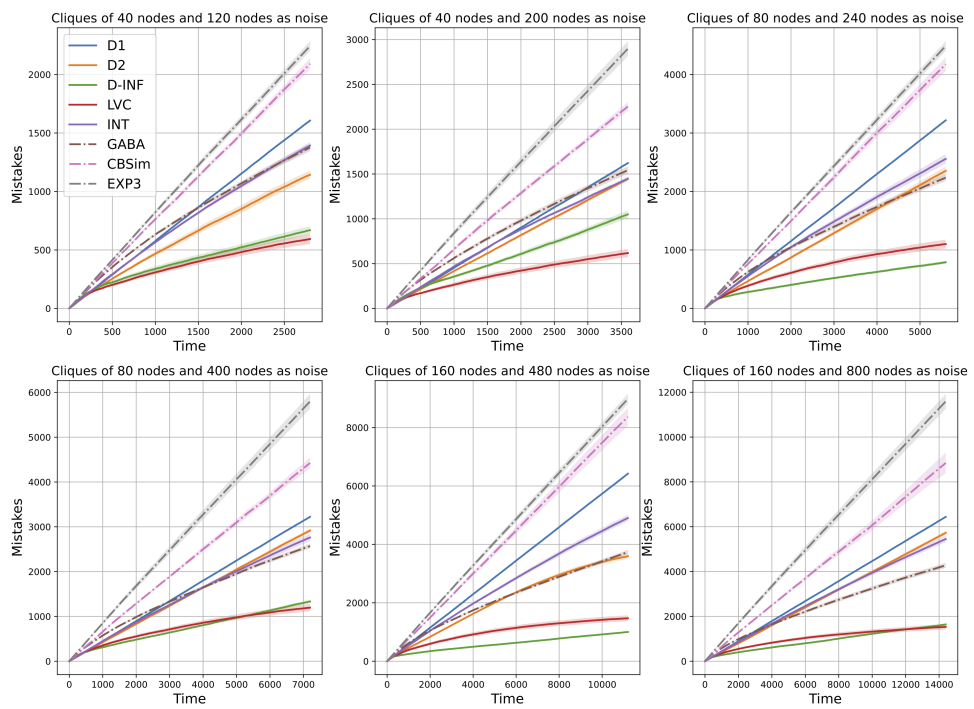


Figure 3: Stochastic Block Model results, dotted lines represent different baselines, while solid lines are used to represent various results.

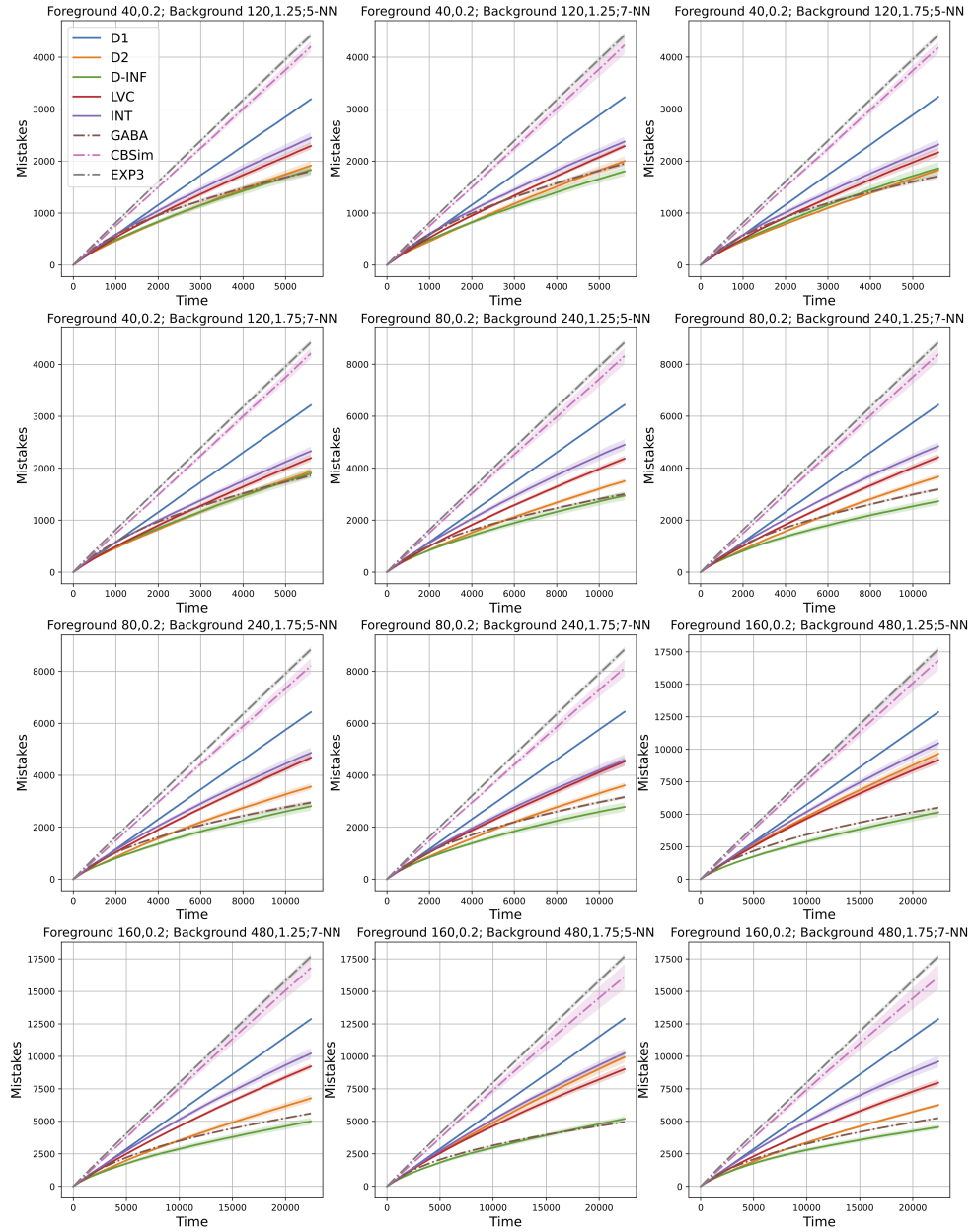


Figure 4: Gaussian graph results, dotted lines represent different baselines, while solid lines are used to represent various results.

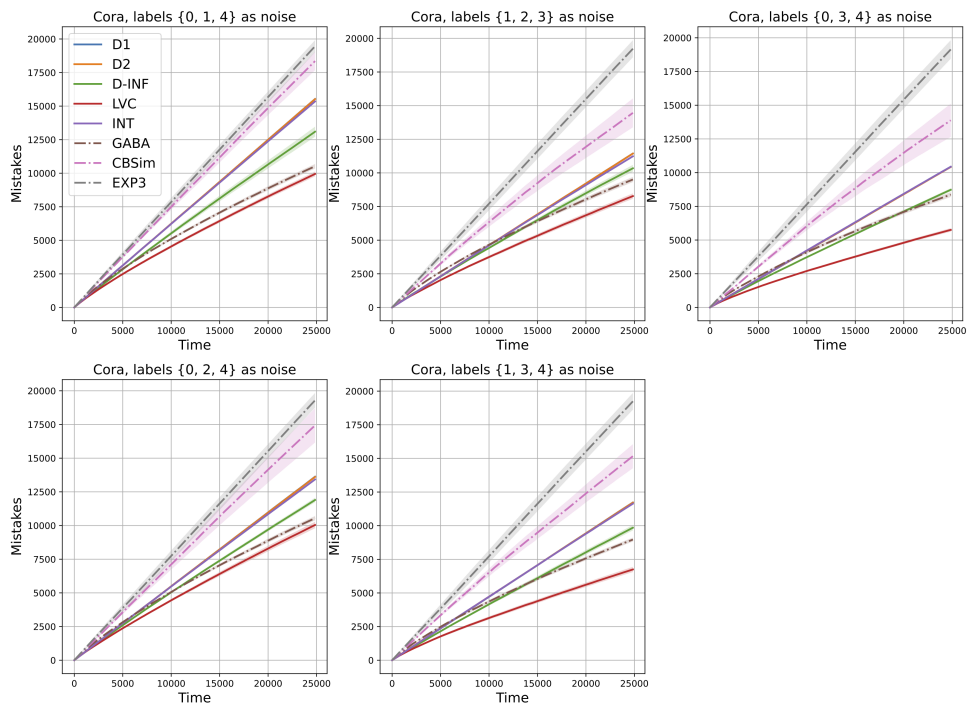


Figure 5: Cora results, dotted lines represent different baselines, while solid lines are used to represent various results

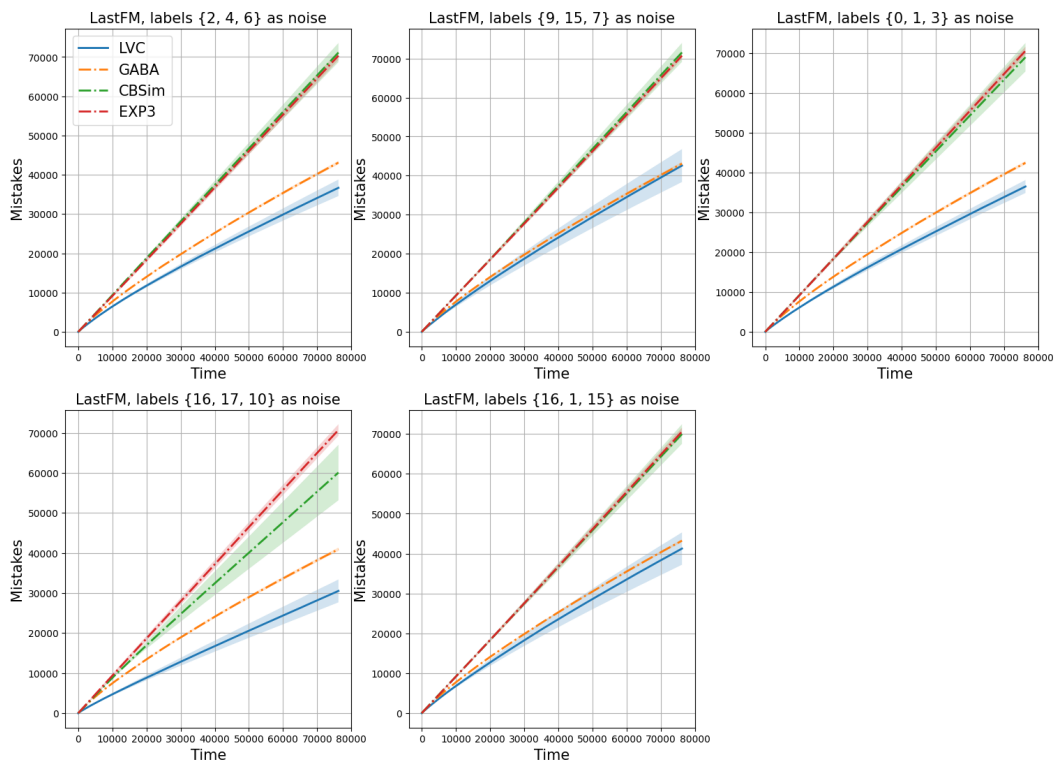


Figure 6: LastFM Asia results, dotted lines represent different baselines, while solid lines are used to represent various results